Sensors and Materials, Vol. 38, No. 11 (2026) 6349–6370
MYU Tokyo

S & M 4685

Examining Step-width Guidance Using a Soft Pneumatic Exosuit via Hip Abduction/Adduction Assistance

Jinnosuke Kamimura, Yuri Mikawa, Tetsuro Miyazaki,* and Kenji Kawashima

Department of Information Physics & Computing, Graduate School of Information Science and Technology, The University of Tokyo, 7-3-1 Hongo, Bunkyo-ku, Tokyo 113-8656, Japan

(Received June 15, 2026; accepted September 24, 2026)

Keywords: soft pneumatic exosuit, pneumatic artificial muscle, human-in-the-loop optimization, step-width guidance, participant experiment

Step-width modulation contributes to mediolateral balance during walking, and soft exosuits are promising for providing step-width guidance with limited interference to natural movement. In a previous study, a human-in-the-loop (HIL) framework based on Bayesian optimization (BO) was proposed for step-width guidance using a soft pneumatic exosuit driven by pneumatic artificial muscles (PAM-SPE). However, its effectiveness was evaluated only in a limited user study ($N = 2$), with analysis restricted to the single factor of assistance condition. In this study, we further evaluated PAM-SPE-based step-width guidance with more participants ($N = 7$) using a two-factor analysis of assistance condition and dynamically varying reference step width (mean ± SD: 0.251 ± 0.061 m). The assistance conditions were initial assistance using the initially obtained parameters, optimized assistance using the parameters obtained via BO, and the unassisted condition. Both assistance conditions significantly outperformed the unassisted condition, while no significant difference was found between the initial and optimized conditions. Post-hoc analysis suggested that assistance was effective for medium-to-large reference step widths, but not for small ones, likely because of physical interference between the PAM-SPE and participants' legs. The BO process in our hip abduction/adduction assistance system also varied across participants, consistent with previous findings on participant-dependent HIL optimization.

1. Introduction

Walking stability is essential for daily mobility, sports activities, and independent living. In gait assistance, balance control is particularly important for older adults because impaired balance is associated with an increased risk of falls.(1) Step width is a representative parameter in mediolateral (ML) balance control,(2) one of the key directions of gait control.(3) Increasing step width enlarges the base of support in the ML direction and can improve robustness against disturbances. However, an excessively large step width increases mechanical and metabolic

*Corresponding author: e-mail: tetsuro_miyazaki@ipc.i.u-tokyo.ac.jp
https://doi.org/10.18494/SAM6483

ISSN 0914-4935 © MYU K.K.
https://myukk.org/

costs and may reduce walking efficiency.[4] Therefore, assisting step-width modulation with the minimum necessary intervention is important for improving ML balance while preserving natural walking.

One promising approach to assisting step-width modulation is the use of a soft pneumatic exosuit (SPE) driven by McKibben-type pneumatic artificial muscles (PAMs).[5,6] PAM-SPE systems are attractive because of their lightweight and compliant characteristics,[7] but their practical implementation faces several challenges. These include the dynamic, adaptive, and difficult-to-model characteristics of the human wearer, as well as the nonlinear and hysteretic behavior of PAMs. In addition, the force transmitted to the body can vary with textile deformation, suit fit, and attachment conditions.[8,9] Responses to haptic assistance can also differ across participants because human motor learning involves sensory integration and error-based adaptation.[10] To address these challenges, a human-in-the-loop (HIL) optimization framework for PAM-SPE was introduced as a complete black box, treating such human–machine systems, which involve numerous interacting components.[11] More broadly, HIL optimization has been widely applied to wearable robotic systems, particularly for gait assistance in the anteroposterior (AP) direction.[12–14] Inspired by these studies, a Bayesian-optimization (BO)-based HIL framework was introduced[11] for the hip abduction/adduction assistance driven by PAM-SPE in the ML direction. In this framework,[11] BO treated the effects of the aforementioned multiple factors as part of a single black-box human–machine system and updated the assistance parameters in real time on the basis of the wearer's actual walking responses. This enabled participant-specific optimization with fewer walking trials, without assuming an explicit analytical model or gradient for these factors.

Although the integrated PAM-SPE system was established in the previous study,[11] it did not provide a detailed user-study evaluation of its guidance effects. Therefore, as an initial step toward future applications in gait assistance, in this study, we further evaluate PAM-SPE-based step-width guidance in seven healthy adults, a larger participant group ($N = 7$) than in the previous study ($N = 2$), using an optimization framework slightly modified on the basis of the insights gained from that study. In particular, we introduce a two-factor statistical analysis that considers both the PAM-SPE assistance condition and the dynamically varying reference step width, whereas in the previous study, only the assistance conditions were compared.[11] This analysis enables us to examine the range of reference step widths over which PAM-SPE-based guidance is effective. We also report that the HIL optimization process in the ML direction differed across participants, consistent with the participant-dependent optimization processes observed in previous HIL optimization studies.[13,14]

The main contributions of this study are as follows.

- We evaluated PAM-SPE-based step-width guidance with a larger participant group ($N = 7$) than in the previous study ($N = 2$).[11]
- We conducted a two-factor statistical analysis incorporating both the assistance condition and the reference step width, enabling the evaluation of the effects of PAM-SPE-based step-width guidance across different reference step widths.
- We confirmed that the BO process varied across participants in the step-width adaptation experiment, consistent with previous findings on participant-dependent HIL optimization processes.[13,14]

The remainder of this paper is organized as follows. Section 2 comprises a description of the materials and methods, including the hardware overview, step width controller, and HIL optimization. The experimental conditions, including the setup, participants, protocol, and statistical analysis, are described in Sect. 3. The experimental results and discussion are presented in Sect. 4. Finally, Sect. 5 concludes the paper.

2. Materials and Methods

In this section, we first describe the hardware configuration of our PAM-SPE, followed by the step-width P controller, HIL optimization, and the experimental procedures.

2.1 Hardware design overview

Figure 1 shows our PAM-SPE used in this study. The exosuit uses the same hardware configuration as that reported in our previous study[11] and is designed to assist step-width modulation by providing hip abduction and adduction assistance during walking. To improve wearability and simplify the mechanical structure, the PAM-SPE covers only the hip region so as not to directly constrain the natural motion of the knee and ankle joints. The suit consists of a waist belt, left and right thigh supporters, and four PAMs anchored to these components. For each leg, one PAM is arranged for hip abduction and another for hip adduction. In particular, the adduction PAMs are arranged in a crossed configuration: the PAM contributing to the left leg is anchored to the right side of the waist belt, whereas the PAM contributing to the right leg is anchored to the left side of the waist belt. Each PAM is individually pressure-controlled by an external servo valve. Details of the hardware, including the dimensions, mass, PAM anchor-point locations, and fixation method, are provided in our previous study.[11]

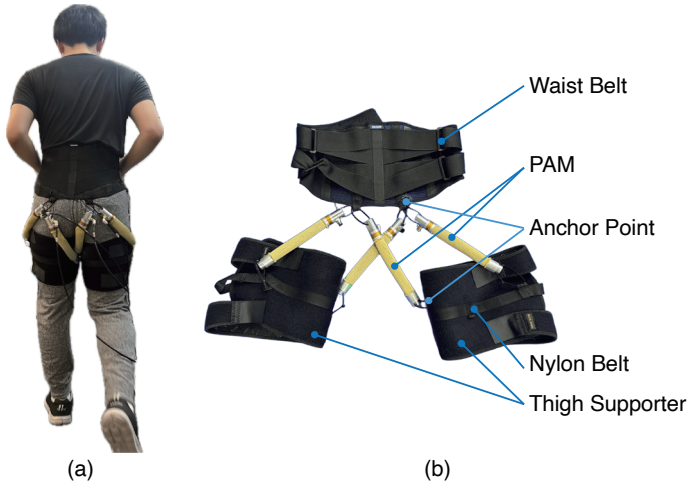


Fig. 1. (Color online) SPE used in this study. (a) Appearance of a person wearing the SPE. (b) Overall configuration of the SPE, consisting of a waist belt, thigh supporters, and PAMs for hip abduction and adduction assistance.

2.2 Step-width P controller

Figure 2 shows the system configuration of the step-width P controller and HIL optimization used in this study. In this study, we designed a P controller for step-width modulation to provide the wearer with haptic feedback corresponding to the step-width error in a more direct and immediate manner. In the previous study,[11] a PI controller was used; however, the integral term tended to accumulate small errors across steps. As a result, assistive force sometimes remained even when the step-width error was small, leading to the excessive correction of the wearer's foot placement. Therefore, in this study, we adopted a P controller for step-width modulation to clarify the relationship between the step-width error and the corresponding assistance.

The input and output variables of the controller are defined using the same framework as in our previous study.[11] Specifically, the foot-position error vector is defined from the difference between the measured ML positions of the left and right feet in the body-centered coordinate system and their corresponding reference positions as $\Delta \boldsymbol{y}^{toe}[k] = \left[\Delta y^{R,toe}[k], \Delta y^{L,toe}[k]\right]^T$. After deadband processing, the effective error vector $\Delta \boldsymbol{y}_{eff}^{toe}[k] = \left[\Delta y_{eff}^{R,toe}[k], \Delta y_{eff}^{L,toe}[k]\right]^T$ is used as the control input. Here, k denotes the discrete time index, and R and L denote the right and left feet, respectively. Detailed definitions of these variables are provided in Appendix 1.

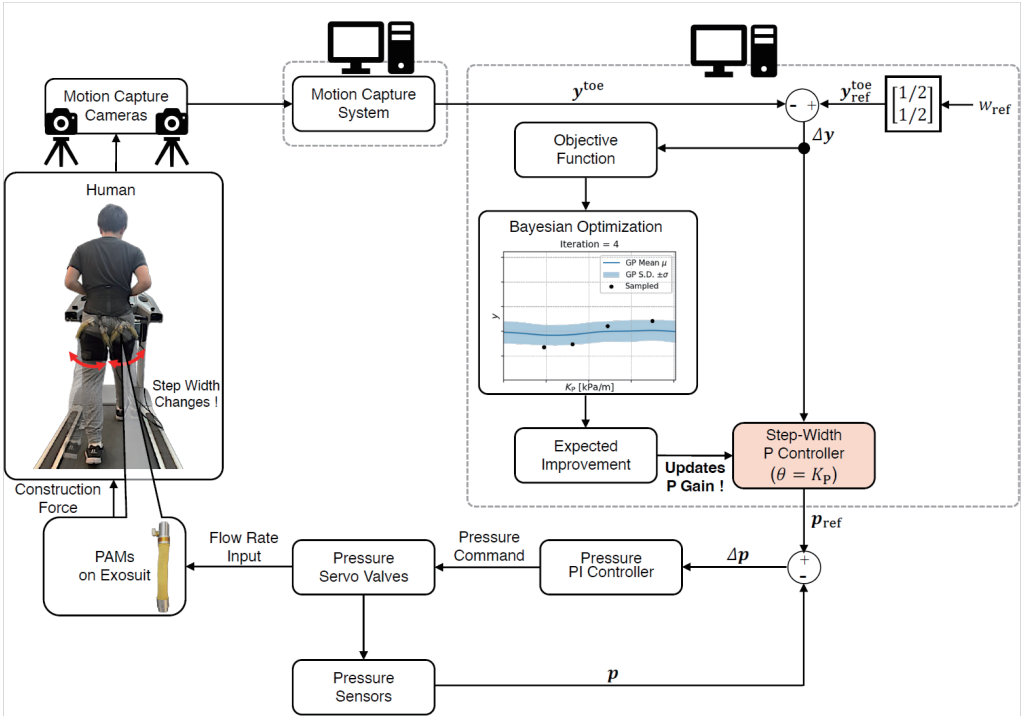


Fig. 2. (Color online) System configuration of the step-width P controller and HIL optimization used in this study. The motion capture system measures the ML foot positions of the wearer, and the step-width error is calculated from the difference between the measured and reference foot positions determined by the reference step width. The step-width P controller converts the step-width error into reference pressures for the PAMs, and the low-level pressure PI controller regulates the servo valves so that the measured pressures track the reference pressures. During HIL optimization, the objective function is calculated from the step-width tracking error, and BO updates the proportional gain K_P referring to the EI criterion.

Depending on the sign of $\Delta \boldsymbol{y}_{eff}^{toe}[k]$, the reference pressure is assigned to either the abduction or adduction PAM for each leg. The reference pressures for the abduction and adduction PAMs are defined as

$$\boldsymbol{p}_{ref}[k] = \begin{bmatrix} p_{ref}^{R,abd}[k] \\ p_{ref}^{R,add}[k] \\ p_{ref}^{L,abd}[k] \\ p_{ref}^{L,add}[k] \end{bmatrix}, \tag{1}$$

where the individual components are given below.

$$p^{s,abd}[k] = \begin{cases} K_P \Delta y_{eff}^{s,toe}[k], & \Delta y_{eff}^{s,toe}[k] > 0 \\ 0, & \Delta y_{eff}^{s,toe}[k] \le 0 \end{cases} \tag{2}$$

$$p^{s,add}[k] = \begin{cases} 0, & \Delta y_{eff}^{s,toe}[k] \ge 0 \\ -K_P \Delta y_{eff}^{s,toe}[k]. & \Delta y_{eff}^{s,toe}[k] < 0 \end{cases} \quad \left(s \in \{R, L\}\right) \tag{3}$$

Here, *abd* and *add* denote abduction and adduction, respectively, and K_p denotes the proportional gain.

As shown in Fig. 2, the generated reference pressure vector $\boldsymbol{p}_{ref}[k]$ is fed into the low-level pressure PI controller. Here, $\boldsymbol{p}[k]$ denotes the actual pressure vector of the PAMs measured by the pressure sensors, and $\Delta \boldsymbol{p}[k] = \boldsymbol{p}_{ref}[k] - \boldsymbol{p}[k]$ denotes the pressure tracking error between the reference and actual pressures. On the basis of this pressure error, the low-level pressure PI controller generates pressure commands for the servo valves so that the internal pressure of each PAM tracks the reference pressure $\boldsymbol{p}_{ref}[k]$.

2.3 HIL optimization

In this study, the proportional gain of the step-width P controller, denoted as $\theta = K_P$, was adjusted for each participant through HIL optimization. The basic concept of sequentially exploring the gain on the basis of step-width tracking performance during actual walking is consistent with the previous study.[11] In contrast, because a P controller is employed for step-width modulation in this study, the optimization variable, objective function, search domain, and step-width tracking task were revised accordingly.

In this study, the wearer's tracking performance was evaluated using a step-width tracking task in which the participant tracked a reference step width updated every 10 s over a 60 s evaluation interval. BO was used for gain tuning, and the gain was sequentially explored so as to minimize the objective function by referring to the step-width error during the task.

For initial sampling, the search domain was divided into four subregions, and one gain was uniformly sampled from each subregion. For each gain, a walking trial was conducted, and the observed value of the objective function was calculated from the step-width error obtained during the evaluation interval. Thereafter, the next gain to be evaluated was selected on the basis of the previously observed data, and the same procedure was repeated. Specifically, the following steps were repeated.

(1) Present assistance using the selected gain.
(2) Execute the reference step-width tracking task.
(3) Measure the objective-function value.
(4) Update the observed data.
(5) Select the next gain to be evaluated.

In this study, the search was conducted for a total of 15 trials, including four initial sampling trials and up to 11 BO trials. The initial best gain was defined as the gain with the minimum objective-function value among the four initial sampling trials. The optimized gain was defined as the gain with the minimum objective-function value among the subsequent 11 BO trials. In the following subsections, the reference step-width tracking task, objective function, search domain, and BO procedure are described in detail.

2.3.1 Step-width tracking task

To evaluate the wearer's ability to track the reference step width, a reference step-width tracking task was defined. Each trial lasted 60 s (Fig. 3). During each trial, the reference step width w_{ref} was presented to the wearer and updated every 10 s. Within each 10 s interval after an update, the reference step width was held constant. The reference step width was set within the allowable range of [0.15, 0.35] m. To avoid presenting similar reference step widths in consecutive intervals, the reference step width was updated such that it remained within the allowable range of 0.15 to 0.35 m and differed from the immediately preceding reference value by at least 0.05 m. At each update time, the next reference step width was determined by uniform sampling from the range satisfying this condition. When the preceding reference value was located near the boundary of the allowable range, sampling was performed from the corresponding nonempty feasible range.

2.3.2 Optimization setup

To quantify step-width tracking performance, an objective function was designed using the foot-placement error at each step during the evaluation interval as a representative measure. Although the foot-position error is defined in continuous time, directly using the continuous-time signal would result in strong autocorrelation among samples and, consequently, redundant evaluation values. Therefore, the heel-strike (HS) timing, at which the foot placement is determined in each gait cycle, was adopted as the representative time point, yielding one HS sample per step. The objective function was defined as the mean squared norm of the foot-position error vectors of the left and right feet at the HS timings, as follows:

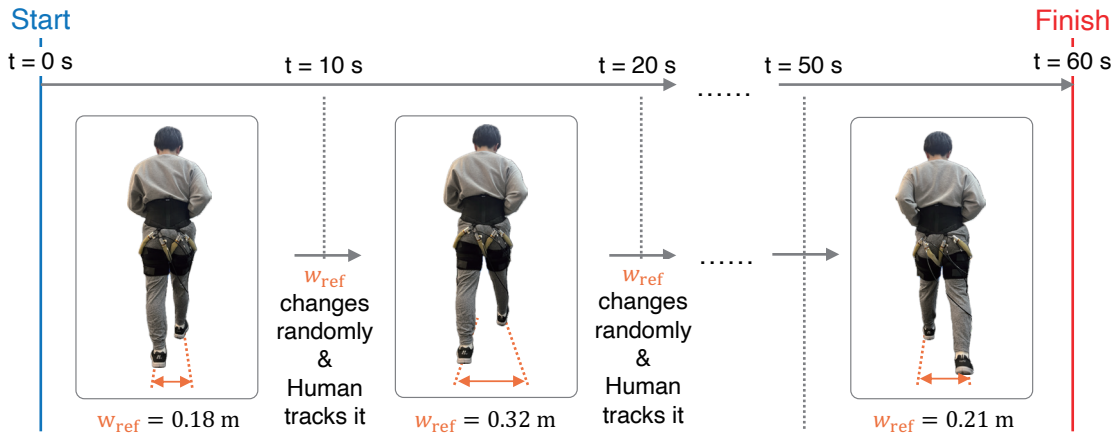


Fig. 3. (Color online) Schematic illustration of the step-width tracking task. During each trial, the reference step width w_{ref} was updated every 10 s. In each interval, the wearer was instructed to track the reference step width on the basis of the haptic guidance provided by the PAM-SPE.

$$f(\theta) = \frac{1}{|\mathcal{I}_{HS}|} \sum_{s\in\{R,L\}} \sum_{k\in\mathcal{I}_{HS}^{s}} \left\| \Delta \boldsymbol{y}^{s,toe}[k] \right\|_2^2, \tag{4}$$

where $\mathcal{I}_{HS}^{s}$ denotes the set of discrete-time indices k at which HS events occur for side $s \in \{R, L\}$. In addition, $\mathcal{I}_{HS} = \bigcup_{s\in\{R,L\}} \mathcal{I}_{HS}^{s}$ denotes the index set of all HS events and $|\mathcal{I}_{HS}|$ represents its cardinality. The search domain was then defined as

$$\Theta = \{\theta = K_P \,|\, 0 \le K_P \le 2.02\times10^{4}\}. \tag{5}$$

The upper bound was determined under the condition that the reference pressure does not exceed the pressure limit p_{lim} = 500 kPa when the control input $\Delta y_{eff}^{s,toe}[k]$ is equal to the deadband width σ_{ML} = 2.47 × 10^{-2} m (Appendix 1), namely,

$$K_P \le \frac{p_{lim}}{\sigma_{ML}}. \tag{6}$$

2.3.3 BO

In BO, the relationship between the objective function and the controller gain is commonly estimated sequentially using a Gaussian process (GP) based on the observed objective-function values, and the next gain to be evaluated is selected using expected improvement (EI) as the acquisition function.[15,16] Following previous studies on HIL optimization for wearable robots, in this study, we also adopted a GP with a radial basis function (RBF) kernel and EI.[13] Considering the participant burden and search efficiency, the search was conducted for a total of 11 trials. After the four initial sampling trials, the observed data were updated, and the next candidate gain was reselected iteratively. The detailed formulation of BO is provided in Appendix 2.

3. Experimental Design

We conducted a user experiment to examine whether the proposed PAM-SPE and gain tuning through HIL optimization support w_{ref} tracking, and whether their effects differ depending on the magnitude of w_{ref}. In this section, we introduce the experimental design.

3.1 Experimental setup

In this study, the body motion of participants walking on a motorized treadmill (Circle Fitness, M7L) was measured. The pneumatic actuation system consisted of four flow-control servo valves (Festo, MPYE-5-1/4-010-B) to which compressed air supplied from a compressor was delivered through an air tank and regulators. These valves were used to individually drive the four PAMs mounted on the suit. Each servo valve was connected to the corresponding PAM through a 4.5m-long polyurethane tube (PISCO, UBT series), and the pressure inside the tubing was measured using a pressure sensor (SMC, PSE510) installed at the output port of each valve.

A motion capture system using Miqus M3 cameras (Qualisys) was employed to measure the participants' body motion. Six cameras were arranged around the treadmill at approximately equal intervals. The three-dimensional coordinates of the markers attached to the participant's body were acquired at a sampling frequency of 500 Hz and transmitted to the control PC via TCP/IP using the dedicated software.

On the control PC (Ubuntu 18.04), the control software was implemented in Python 2.7 and C++ 14 on ROS Melodic. The step-width P controller and the BO algorithm were executed on this system. GPyOpt[17] was used for the implementation of BO. All sensor and control signals were recorded as logs and used for offline objective-function evaluation and statistical analysis.

3.2 Participants

Seven healthy adult male participants took part in this study (age: 23 ± 1.2; body mass: 65 ± 4.9 kg; height: 1.71 ± 0.10 m; *mean* ± *S.D.*). The study protocol was approved by the Ethics Committee of the Graduate School of Information Science and Technology, The University of Tokyo (approval number: UT-IST-RE-250402-2). Written informed consent was obtained from all participants before the experiment. After the experiment, each participant received compensation equivalent to US$ 24.92 (4000 JPY in local currency).

3.3 Experimental protocol

The participant experiment in this study consisted of three sessions conducted on the same day: an adaptation session, a parameter-tuning session, and a validation session. In all sessions, the participants walked on the treadmill, and the walking speed was kept constant at 4.0 km/h throughout the experiment.

To reduce variability in participants' responses to the assistance, the following common instructions were verbally provided immediately before the experiment:

(a) The presented reference step width should be regarded as a guide rather than a value to be matched exactly.
(b) The participants should not excessively resist the lateral guidance provided by the suit and should walk at a natural rhythm.
(c) The participants should immediately report any pain, numbness, strong discomfort, or fear. (There was no opt-out during the actual experiment.)

3.3.1 Adaptation session

First, an adaptation session was conducted to allow the participants to become sufficiently accustomed to walking on the treadmill while wearing the PAM-SPE. The participants wore the PAM-SPE, and step-width guidance was provided using a proportional gain that had been tuned in preliminary experiments to ensure stable operation. The participants continued walking until they verbally reported that they could walk without discomfort. During this period, it was confirmed that there was no displacement of the motion-capture markers or interference from the pneumatic tubing.

3.3.2 Parameter-tuning session

Next, a parameter-tuning session was conducted to identify a suitable proportional gain for each participant through HIL optimization. In this session, as described in Sect. 2.3, the participants performed four initial sampling trials followed by up to 11 trials using the BO process. To avoid redundant evaluations, BO was terminated when the distance between two consecutive candidate gains fell below 1.0×10^{-8}.

3.3.3 Validation session

Finally, a validation session was conducted to evaluate the effectiveness of the proportional gain obtained through optimization. In the validation session, the following three conditions were used.

(a) Unassisted condition

The participant wore the PAM-SPE, but the PAMs were not actuated. Because no haptic guidance was provided under this condition, the reference step width was presented in real time using a custom-built tablet application through both visual and auditory cues, as shown in Fig. 4. The tablet device was placed in front of the participant so that the participant could check the reference step width while maintaining a forward gaze.

(b) Initial best condition

Assistance was provided by the PAM-SPE using the initial best gain, defined as the proportional gain that yielded the minimum objective-function value among the four initial

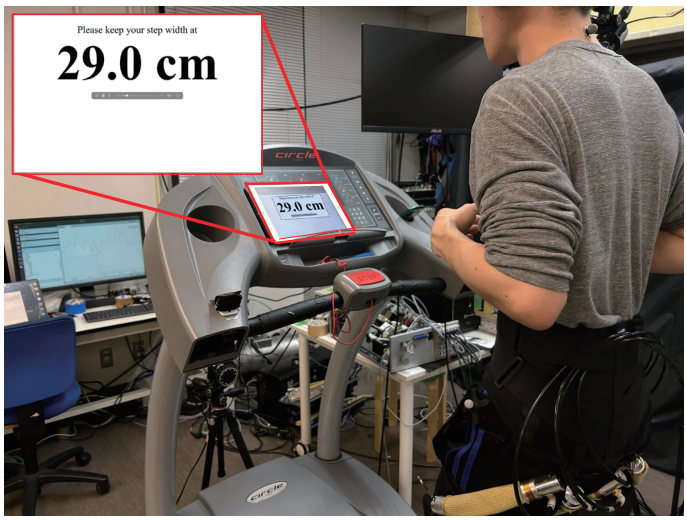


Fig. 4. (Color online) Appearance of the custom-built tablet application, placed at the console of the treadmill, under the unassisted condition during the validation session. In the application, the reference step width was displayed in centimeters in real time, via both visual and auditory cues.

sampling trials in the parameter-tuning session. No visual or auditory cues regarding the reference step width were provided under this condition; the participant received step-width guidance solely through the haptic assistance generated by the PAM-SPE. To reduce the effect of the operating noise of the servo valves, the participants wore headphones and listened to white noise so that ambient sounds were masked.

(c) Optimized condition

Assistance was provided by the PAM-SPE using the optimized gain, defined as the proportional gain that yielded the minimum objective-function value among the BO trials completed after the initial sampling in the parameter-tuning session. As in the initial best condition, no visual or auditory cues regarding the reference step width were provided, and step-width guidance was delivered solely through the haptic assistance generated by the PAM-SPE. The participants also listened to white noise through headphones to mask the operating noise of the servo valves.

The order of the three conditions was determined using a Latin square design, and three walking trials were conducted for each condition. To reduce carryover effects between conditions and trials, sufficient rest periods were provided between trials, and the experiment was conducted while confirming the participants' subjective fatigue and discomfort. The entire experiment required approximately 1.5 h to complete.

3.4 Evaluation metrics and preprocessing

To evaluate whether the proposed method improved the wearer's ability to track the reference step width, the root mean square error (*RMSE*) between the reference step width w_{ref} and the

measured step width w across each 10 s segment was used as the evaluation metric. As preprocessing, a first-order low-pass filter with a cutoff frequency of 10 Hz was applied to the signals, after which the data were downsampled from 500 to 100 Hz. The middle 60 s of each 90 s trial was then extracted as the analysis interval.

To examine whether the tracking error varied with the magnitude of the reference step width, the analysis interval for each trial was divided into 10 s segments, during which the reference step width was held constant. The step-width *RMSE* was calculated for each segment, and the reference step width w_{ref} presented during that interval was assigned to the corresponding segment. The *RMSE* for condition c and segment j was then defined as

$$RMSE_{c,j} = \sqrt{\frac{1}{\left|\mathcal{I}_{c,j}\right|} \sum_{k \in \mathcal{I}_{c,j}} \left(w_{ref,j} - w[k]\right)^2}, \tag{7}$$

where $\mathcal{I}_{c,j}$ denotes the set of discrete-time indices k included in the jth segment under condition c, and $\left|\mathcal{I}_{c,j}\right|$ denotes the number of samples in that segment. In addition, $w_{ref,\,j}$ denotes the reference step width presented during the jth segment.

3.5 Statistical analysis

A linear mixed model (LMM) was used to analyze the step-width *RMSE* as the response variable, with condition c, reference step width w_{ref}, and their interaction included as fixed effects.[18] To account for within-participant repeated measurements, a random intercept for each participant was included in the model. By treating reference step width as a continuous predictor, the LMM enabled us to examine how the effect of the assistance condition varied across reference step widths without discretizing the reference values into categories.

The interaction between condition and reference step width was examined by calculating estimated marginal means (EMMs) for each condition at representative values of w_{ref}, using the fitted LMM. These representative values were objectively selected as $\mu_{w_{ref}} - \sigma_{w_{ref}}$, $\mu_{w_{ref}}$, and $\mu_{w_{ref}} + \sigma_{w_{ref}}$ to characterize the effect of the continuous covariate at lower, average, and higher levels, rather than by arbitrarily discretizing it into groups. Here, $\mu_{w_{ref}}$ and $\sigma_{w_{ref}}$ respectively denote the mean and standard deviation (S.D.) of the reference step width across all participants.

When the fixed-effect test indicated a significant interaction between condition and reference step width, pairwise comparisons among conditions were performed at each representative value. The pairwise comparisons were based on the EMMs, and Holm correction was applied to the three comparisons within each representative value.

4. Results and Discussion

4.1 Optimization of the proportional gain

Figure 5 shows the progression of the objective-function observations [Eq. (4)] during representative parameter-tuning sessions. Figures 5(a) and 5(b), corresponding to Subjects 2 and

3, respectively, show representative cases in which BO yielded observations with objective-function values smaller than those obtained during the initial sampling trials. Figure 5(c) shows the result for Subject 4, representing a case in which BO did not improve upon the initial best objective-function value. Subjects 2 and 3 represent successful BO cases, whereas Subject 4 represents a case in which BO did not outperform the initial sampling result. In five of the seven participants, objective-function values smaller than the minimum obtained during initial sampling were observed during the BO process, except for Subjects 1 and 4. The objective-function observation corresponding to the initial best gain and the optimized gain for each participant are provided in Appendix 3.

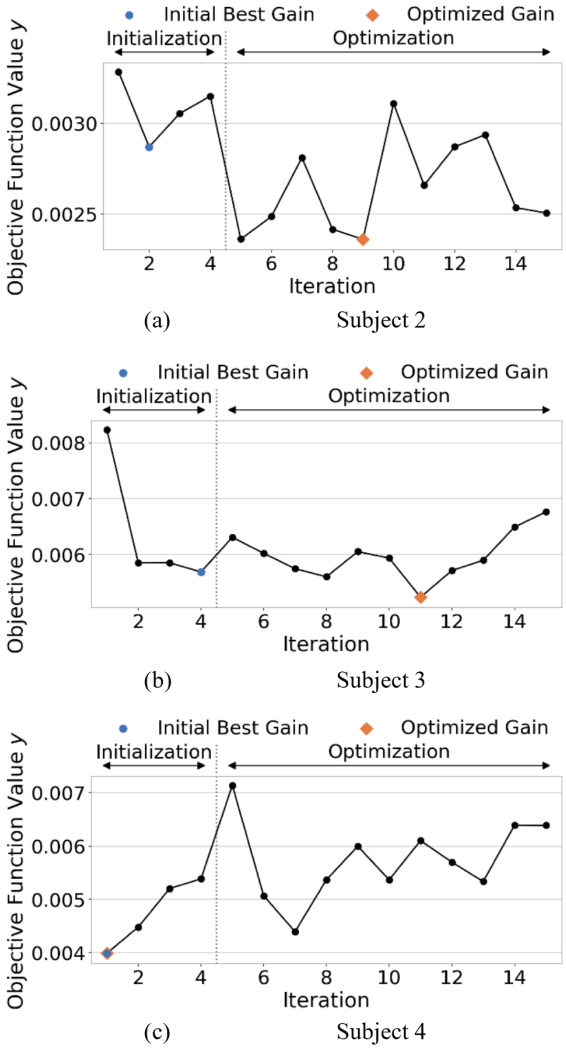


Fig. 5. (Color online) Objective-function observations [Eq. (4)] during BO for Subjects (a) 2, Subject (b) 3, and (c) 4. Blue circles indicate the initial best gain, whereas orange diamonds indicate the optimized gain. Panels (a) and (b) show representative examples in which BO yielded objective-function observations lower than those obtained during the initial sampling trials, whereas panel (c) shows a representative example in which BO did not yield an observation lower than that obtained with the initial best gain. The first four evaluations correspond to the initial sampling trials, and the proportional gain was sequentially updated by BO from the fifth evaluation onward.

Figure 6 shows the final objective-function landscapes [Eq. (4)] obtained through BO. The objective-function landscapes differed across participants, suggesting that the effect of a given proportional gain on the step-width tracking error varied among participants. This finding is consistent with the previous observation that wearing conditions and force-transmission characteristics differ across participants.[11] In addition, for many participants, the sampling points were concentrated near the optimized gain, indicating that BO explored gain regions suited to each participant.

Figure 7 shows the initial best and optimized gains for each participant. For Subject 1, BO was terminated early because the distance between two consecutive candidate gains fell below

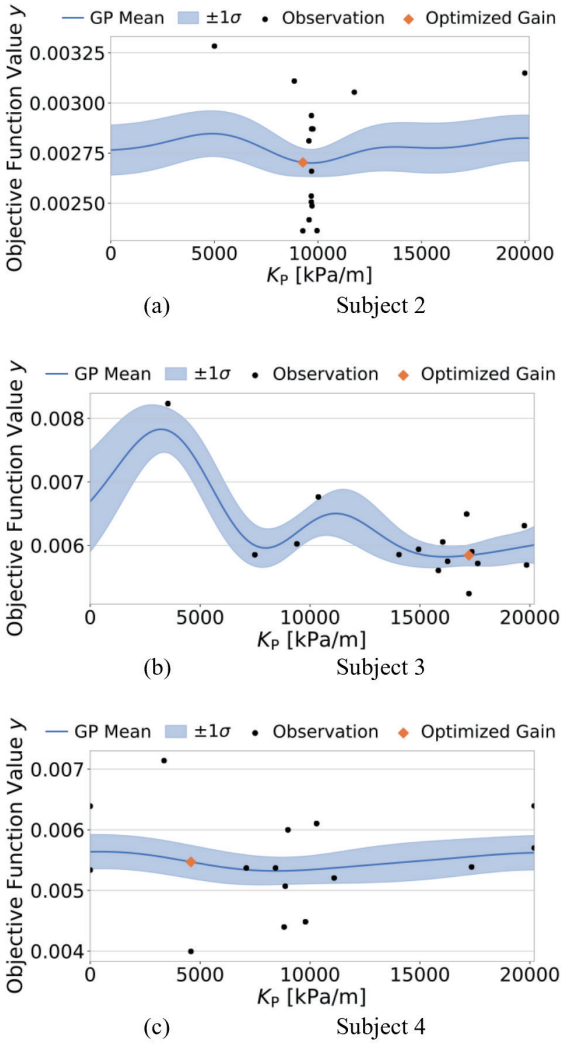


Fig. 6. (Color online) Objective-function landscapes [Eq. (4)] during BO for Subjects (a) 2, (b) 3, and (c) 4. Solid lines indicate the posterior mean of the GP for the objective function, and shaded regions indicate the posterior S.D. Orange diamonds indicate the optimized gain. Although the objective-function landscapes differed across participants, as shown in panels (a) and (b), the sampling points were concentrated near the optimized gain for many participants. However, as shown in panel (c), there was also a case in which the sampling points were not concentrated near the optimized gain.

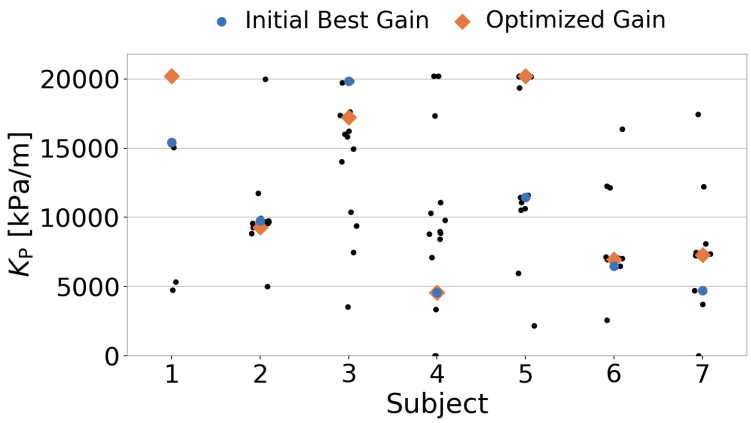


Fig. 7. (Color online) Proportional gains evaluated during the parameter-tuning session for each participant. Black dots indicate the candidate gains evaluated during optimization. Blue circles indicate the initial best gain and orange diamonds indicate the optimized gain.

the predefined stopping threshold. The optimized gain differed across participants, which is consistent with previous studies, and shows that HIL optimization for wearable robots identifies participant-specific control parameters. In addition, for Subjects 1 and 5, the optimized gain reached the upper bound of the search domain [Eq. (5)] (2.02×10^4 kPa/m). This result suggests that, for some participants, a larger proportional gain or greater assistance force than that allowed by the search range used in this study may be effective.

To compare the differences between these gains, the absolute difference between the initial best and optimized gains for each participant was normalized by the width of the proportional-gain search domain. The normalized gain difference was 16.9 ± 14.2% (*mean* ± *S.D.*). The two gains were relatively similar for some participants, whereas larger differences were observed for others. The similarity between the two gains for some participants may partly reflect the BO search process used in this study. The EI acquisition function selects the next evaluation point on the basis of both the predicted objective-function value and its uncertainty. Therefore, regions around gains that yielded favorable objective-function values during the initial sampling may remain candidates for subsequent exploration during BO. Whether the optimized gain provides higher step-width tracking performance than the initial best gain is evaluated in the statistical analysis in the next section.

4.2 Statistical analysis of user-study results

The fixed-effect tests in the LMM showed no significant main effect of reference step width [$F(1, 366.14) = 0.231$, $p = 0.631$]. In contrast, a significant main effect of condition was observed [$F(2, 366.17) = 9.809$, $p < 0.001$], and the interaction between reference step width and condition was also significant [$F(2, 366.17) = 14.99$, $p < 0.001$]. These results indicate that the effect of the assistance condition on step-width *RMSE* varied depending on the magnitude of the reference step width.

Because the interaction was significant, pairwise comparisons among conditions were performed at each representative value of the reference step width. These comparisons were based on the EMMs shown in Fig. 8, where $\mu_{w_{ref}} = 0.251$ m and $\sigma_{w_{ref}} = 0.061$ m. The Holm correction was applied to the three comparisons at each representative value.

At the lower representative value of w_{ref} $(\mu_{w_{ref}} - \sigma_{w_{ref}})$, no significant differences were found among the conditions. In contrast, at the average representative value $(\mu_{w_{ref}})$, the *RMSE* values under the initial best and optimized conditions were significantly smaller than those under the unassisted condition ($z = 2.606$, $p = 0.018$ and $z = 3.990$, $p < 0.001$, respectively), while no significant difference was found between the initial best and optimized conditions ($z = 1.387$, $p = 0.166$). Similarly, at the higher representative value $(\mu_{w_{ref}} + \sigma_{w_{ref}})$, the *RMSE* values under the initial best and optimized conditions were significantly smaller than those under the unassisted condition ($z = 5.301$, $p < 0.001$ and $z = 5.969$, $p < 0.001$, respectively), while no significant difference was found between the initial best and optimized conditions ($z = 0.827$, $p = 0.408$).

Taken together, these results indicate that the step-width guidance provided by the proposed PAM-SPE improved the step-width tracking performance across participants at average and large reference step widths. However, no significant improvement was observed at a small reference step width, suggesting that the assistance effect was not uniform across reference step widths but depended on the magnitude of the reference step width. In addition, no statistically significant additional improvement under the optimized condition over the initial best condition was confirmed.

4.2.1 Considerations on the effect of PAM assistance

At the lower representative value of w_{ref} $(\mu_{w_{ref}} - \sigma_{w_{ref}})$, no significant reduction in *RMSE* relative to the unassisted condition was observed under either the initial best or optimized

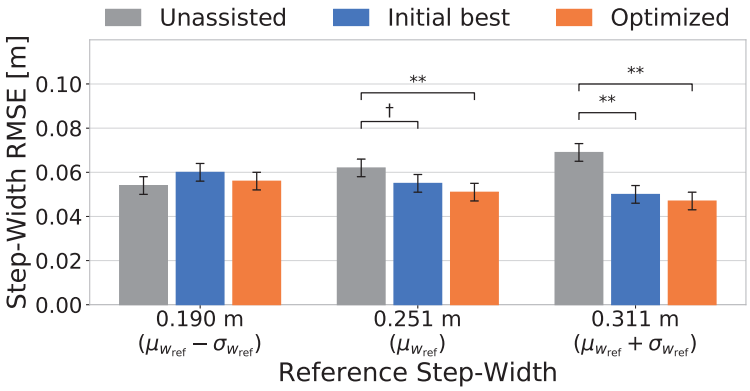


Fig. 8. (Color online) Step-width *RMSE* across reference step-width levels under unassisted, initial best, and optimized conditions. Values indicate the EMMs obtained from the LMM and error bars represent standard errors. Brackets indicate pairs for which significant differences were found in Holm-adjusted pairwise comparisons against the unassisted condition ($^{\dagger}p < .05$, $^{*}p < .01$, $^{**}p < .001$).

condition. This may be attributed to the mechanical constraint imposed by the suit's structure. In the PAM-SPE used in this study, the PAMs for hip adduction were arranged to cross between the left and right sides. In addition, when pressurized, the PAMs contract in the axial direction while expanding in the radial direction. Therefore, under the small-reference-step-width condition, the crossed PAMs were observed, in some cases, to become bulky around the thighs during actuation, making it difficult for the participants to take a narrow step. Such structural interference may have made the assistance effect less likely to appear as a reduction in *RMSE* at relatively small reference step widths.

In contrast, at the average and higher representative values of w_{ref} ($\mu_{w_{ref}}$ and $\mu_{w_{ref}} + \sigma_{w_{ref}}$, respectively), the *RMSE* values under the initial best and optimized conditions were significantly smaller than those under the unassisted condition. Previous work has shown that, during walking with a wide step, the characteristics of foot-placement control change and kinematic variability increases.[19] Therefore, under conditions with large reference step widths, ML foot-placement corrections larger than those required during normal walking may have been necessary, making tracking errors more likely to increase when relying only on voluntary foot-placement control. Under such conditions, the proposed method, which provides hip abduction/adduction assistance based on the step-width error, may have supported correcting foot placement and suppressed the increase in *RMSE*.

Post-stroke individuals have been reported to adopt a wider step as a compensatory strategy for maintaining walking stability.[20] However, walking with a step width greater than the preferred width increases metabolic cost.[4] These findings suggest that simply increasing step width may not always be desirable and that guiding step width according to individual gait characteristics may be meaningful for gait training. In this study, significant reductions in tracking error were observed at the average and higher representative values of the reference step width. Given that post-stroke individuals tend to adopt relatively wide steps, these results suggest that the proposed method may be applicable to guiding step width from larger values toward a more moderate target in post-stroke gait training.

These results suggest that hip abduction/adduction assistance may have contributed to correcting foot placement. However, walking involves the coordinated motion of multiple joints, including not only the hip but also the knee and ankle joints.[21] Therefore, it is also necessary to consider how the hip assistance used in this study affected the motion of these other joints. Since the effects on knee and ankle joint motion were not quantitatively evaluated in this study, future work should assess, from a biomechanical perspective, whether these joints maintain natural joint motion and appropriate ranges of motion during walking.

4.2.2 Considerations on the effect of the proposed BO

There was no significant difference between the initial best and optimized conditions. Thus, it cannot be concluded that the optimized gain provided performance statistically superior to that of the initial best gain.

One possible reason for this result is that the signal-to-noise ratio of the objective-function observations was relatively low. Previous HIL optimization studies also revealed that BO must identify near-optimal control parameters from noisy physiological measurements, such as metabolic cost, within a limited number of trials. However, the objective function used in this study may have had an even lower signal-to-noise ratio than such physiological measures because it was based on step-width error, which directly reflects the process by which participants voluntarily attempted to match the reference step width.[14] Therefore, even under the same proportional gain, the evaluation value may have varied depending on factors unrelated to the gain itself, such as changes in gait strategy, fatigue, attention, and compensatory movements for maintaining stability. Such variability may have reduced the reliability of the objective-function observations and made it difficult for BO to identify an optimized gain that was statistically superior to the initial best gain.

These findings suggest that, when applying HIL optimization to tasks such as step-width tracking, in which voluntary control and stability control are strongly involved, temporal variations in objective function and within-participant variability can be important challenges. Nevertheless, the results under the optimized condition showed a significantly lower *RMSE* than those under the unassisted condition at relatively large reference step widths. Thus, the optimized gain selected through the proposed HIL optimization approach may be a promising means of suppressing increases in step-width *RMSE* under conditions in which step-width tracking becomes difficult. In addition, if BO-HIL can identify control parameters suited to each individual within a limited number of trials, it may reduce the burden of adjusting assistance conditions in clinical settings. However, this study did not directly evaluate whether the number of trials required for optimization could be reduced; therefore, further investigation is needed.

5. Conclusions

In this study, building on the gait-guidance control framework using the PAM-SPE proposed in the previous work,[11] we revised the step-width controller and the HIL optimization configuration. Then, the effectiveness of the proposed method was further evaluated through experiments with seven participants.

The results indicate that the proposed PAM-based hip abduction/adduction assistance can improve step-width tracking performance, particularly for medium-to-large reference step widths, while the assistance effect in the small step-width range may have been limited owing to the mechanical interference of PAMs. By contrast, the BO of proportional gain did not yield an optimized gain that was statistically superior to the initial best gain. This may be because the objective function has been affected by multiple factors, such as voluntary foot-placement adjustment, gait adaptation, fatigue, and compensatory movements for maintaining stability, which were not explicitly accounted for in the function. In addition, the optimized gain reached the upper limit of the search range for some participants, suggesting that a wider assistance range or a larger achievable assistance force may be beneficial. Nevertheless, BO identified participant-specific gains and enabled systematic tuning without requiring manual parameter adjustment.

Future work should include refining the objective function to account for fatigue and gait adaptation, and improving the suit structure to reduce mechanical interference, especially under small step-width conditions.

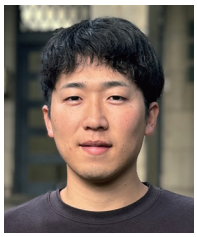
Acknowledgments

The authors would like to thank Bridgestone Corporation for providing the PAMs used in this study. This research was supported by JSPS KAKENHI Grant Number JP25K14762.

References

1 D. L. Sturnieks, R. St George, and S. R. Lord: Neurophysiol. Clin. **38** (2008) 467. https://doi.org/10.1016/j.neucli.2008.09.001
2 A. D. Kuo: Int. J. Robot. Res. **18** (1999) 917. https://doi.org/10.1177/02783649922066655
3 M. H. Woollacott and P. F. Tang: Phys. Ther. **77** (1997) 646.
4 J. M. Donelan, R. Kram, and A. D. Kuo: Proc. R. Soc. Lond. B Biol. Sci. **268** (2001) 1985. https://doi.org/10.1098/rspb.2001.1761
5 C. P. Chou and B. Hannaford: IEEE Trans. Robot. Autom. **12** (1996) 90. https://doi.org/10.1109/70.481753
6 B. Tondu and P. Lopez: IEEE Control Syst. Mag. **20** (2000) 15. https://doi.org/10.1109/37.833638
7 M. Wehner, B. Quinlivan, P. M. Aubin, E. Martinez-Villalpando, M. Baumann, L. Stirling, K. Holt, R. Wood, and C. Walsh: Proc. 2013 IEEE Int. Conf. Robot. Autom. (IEEE, 2013) 3362–3369. https://doi.org/10.1109/ICRA.2013.6631046
8 T. Miyazaki, T. Tagami, D. Morisaki, R. Miyazaki, T. Kawase, T. Kanno, and K. Kawashima: Appl. Sci. **9** (2019) 2869. https://doi.org/10.3390/app9142869
9 M. B. Yandell, B. T. Quinlivan, D. Popov, C. Walsh, and K. E. Zelik: J. NeuroEngineering Rehabil. **14** (2017) 40. https://doi.org/10.1186/s12984-017-0247-9
10 D. Wolpert, J. Diedrichsen, and J. Flanagan: J. Nat Rev Neurosci. **12** (2011) 739. https://doi.org/10.1038/nrn3112
11 J. Kamimura, T. Miyazaki, and K. Kawashima: Proc. 2026 IEEE/SICE Int. Symp. Syst. Integr. (IEEE, 2026) 358–363. https://doi.org/10.1109/SII64115.2026.11404503
12 J. Zhang, P. Fiers, K. A. Witte, R. W. Jackson, K. L. Poggensee, C. G. Atkeson, and S. H. Collins: Science **356** (2017) 1280. https://doi.org/10.1126/science.aal5054
13 Y. Ding, M. Kim, S. Kuindersma, and C. J. Walsh: Sci. Robot. **3** (2018) eaar5438. https://doi.org/10.1126/scirobotics.aar5438
14 D. F. N. Gordon, C. McGreavy, A. Christou, and S. Vijayakumar: IEEE Trans. Robot. **38** (2022) 1410. https://doi.org/10.1109/TRO.2021.3133137
15 E. Brochu, V. M. Cora, and N. de Freitas: arXiv:1012.2599 (2010). https://arxiv.org/abs/1012.2599.
16 P. I. Frazier: arXiv:1807.02811 (2018). https://arxiv.org/abs/1807.02811
17 The GPyOpt authors: GPyOpt: A Bayesian Optimization Framework in Python http://github.com/SheffieldML/GPyOpt (accessed April 2026).
18 D. Bates, M. Mächler, B. Bolker, and S. Walker: J. Stat. Software **67** (2015) 1. https://doi.org/10.18637/jss.v067.i01
19 J. A. Perry and M. Srinivasan: R. Soc. Open Sci. **4** (2017) 160627. https://doi.org/10.1098/rsos.160627
20 A. C. Dragunas, T. Cornwell, R. López-Rosado, and K. E. Gordon: IEEE Trans. Neural Syst. Rehabil. Eng. **29** (2021) 731. https://doi.org/10.1109/TNSRE.2021.3072252
21 D. A. Winter: Gait Posture **3** (1995) 193. https://doi.org/10.1016/0966-6362(96)82849-9

About the Authors



Jinnosuke Kamimura received his B.E. degree in engineering from Tokyo University of Agriculture and Technology, Japan, in 2024 and his M.S. degree in information science and technology from The University of Tokyo, Japan, in 2026. Since 2026, he has been pursuing a Ph.D. degree at The University of Tokyo, Japan. His research interests include mechanical engineering, control engineering, wearable power-assistive devices, and surgical robotics. (5158231060kj@g.ecc.u-tokyo.ac.jp)



Yuri Mikawa received her BE, ME, and PhD degrees in information science and technology from The University of Tokyo, Japan, in 2018, 2020, and 2023, respectively. She was a guest doctorate at the Technical University of Munich, Germany, from 2022 until 2023. She is currently an assistant professor at The University of Tokyo, Japan. Her research interests include the virtual/augmented reality display of aerial images and projection mapping with high-speed vision and visual perception. (yurimikawa@g.ecc.u-tokyo.ac.jp)



Tetsuro Miyazaki received his Ph.D. degree in engineering from the Department of Mechanical Sciences and Engineering, Tokyo Institute of Technology, in 2014. He was a research assistant from 2014 to 2015, and an assistant professor with Yokohama National University from 2015 to 2017. From 2017 to 2020, he was an assistant professor with Tokyo Medical and Dental University. From 2020 to 2021, he was an assistant professor with the Graduate School of Information Science and Technology, The University of Tokyo. Since January 2022, he has been a lecturer with the same institution. His research interests include mechanical engineering, control engineering, power-assistive devices, and medical welfare robotics.
(tetsuro_miyazaki@ipc.i.u-tokyo.ac.jp)



Kenji Kawashima received his Ph.D. degree in engineering from the Department of Control Engineering, Tokyo Institute of Technology, Tokyo, Japan, in 1997. From 1997 to 2000, he was a research assistant with the Tokyo Metropolitan College of Industrial Technology. He was an associate professor with the Precision and Intelligence Laboratory, Tokyo Institute of Technology, from 2000 to 2013. From 2013 to 2020, he was a professor with Tokyo Medical and Dental University. In 2014, he founded a university start-up, Riverfield Inc. Since April 2020, he has been a professor with The University of Tokyo. His research interests include bio-robotic control, soft actuators, medical imaging and the measurement and control of a fluid system.
(kenji_kawashima@ipc.i.u-tokyo.ac.jp)

Appendix

Appendix 1: Definition of Step-width Error and Deadband Processing

To achieve step-width modulation, the control error was defined as the difference between the ML position of the foot and its reference position in the trunk-centered coordinate system. In this study, using the marker measurements shown in Fig. 9, a trunk-centered coordinate system was defined with its origin at the umbilical position. The foot-position vector, whose components are the ML coordinates of the right and left toe markers in this coordinate system, was defined as

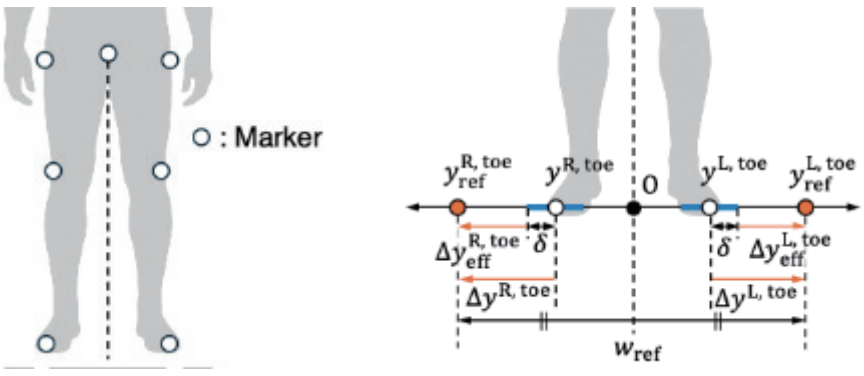
$$\boldsymbol{y}^{toe}[k] = \begin{bmatrix} y^{R,toe}[k] \\ y^{L,toe}[k] \end{bmatrix}. \tag{8}$$

The reference foot-position vector corresponding to the reference step width w_{ref} was defined as

$$\boldsymbol{y}_{ref}^{toe}[k] = \begin{bmatrix} y_{ref}^{R,toe}[k] \\ y_{ref}^{L,toe}[k] \end{bmatrix} = w_{ref} \begin{bmatrix} \frac{1}{2} \\ \frac{1}{2} \end{bmatrix}. \tag{9}$$

The step-width error vector $\Delta\boldsymbol{y}^{toe}[k]$ was then defined as

$$\Delta\boldsymbol{y}^{toe}[k] = \boldsymbol{y}_{ref}^{toe}[k] - \boldsymbol{y}^{toe}[k]. \tag{10}$$



(a) (b)

Fig. 9. (Color online) Marker placement and definitions of step width and foot-position coordinates. (a) Marker placement used for motion capture. (b) Definition of the trunk-centered coordinate system and variables used to calculate the step-width error. Here, O denotes the origin of the trunk-centered coordinate system, w_{ref} denotes the reference step width, and $y^{s,toe}$ and $y_{ref}^{s,toe}$ denote the ML and reference positions of the toe marker, respectively. $\Delta y^{s,toe}$ denotes the step-width error and $\Delta y_{eff}^{s,toe}$ denotes the effective error after applying the deadband width δ, where $s \in \{R, L\}$.

For each component $\Delta y^{s,toe}[k]$ ($s \in \{R, L\}$), $\Delta y^{s,toe}[k] > 0$ indicates an error in the abduction direction, whereas $\Delta y^{s,toe}[k] < 0$ indicates an error in the adduction direction.

Furthermore, to avoid excessive assistance in response to small fluctuations associated with natural walking, a deadband width δ was introduced. The effective error vector $\Delta \boldsymbol{y}_{eff}^{toe}[k]$ was defined as

$$\Delta \boldsymbol{y}_{eff}^{toe}[k] = \begin{bmatrix} \Delta y_{eff}^{R,toe}[k] \\ \Delta y_{eff}^{L,toe}[k] \end{bmatrix}. \tag{11}$$

Each component was defined as

$$\Delta y_{eff}^{s,toe}[k] = \begin{cases} \Delta y^{s,toe}[k], & \left|\Delta y^{s,toe}[k]\right| > \delta \\ 0. & \left|\Delta y^{s,toe}[k]\right| \le \delta \end{cases} \quad \left(s \in \{R, L\}\right) \tag{12}$$

The deadband width was set to $\delta = \sigma_w / \sqrt{2} \simeq 2.47 \times 10^{-2}$ m on the basis of the step-width S.D. σ_w = 0.035 m reported by Perry and Srinivasan.[19]

Appendix 2: Detailed Formulation of BO

Surrogate model based on GP regression

In BO, instead of directly using the objective function $f(\theta)$, a surrogate model is constructed using GP, which is a probabilistic model. The observation y is assumed to be the true function value $f(\theta)$ corrupted by the additive Gaussian noise ε and is given as[15,16]

$$y = f(\theta) + \varepsilon, \qquad \varepsilon \sim N\left(0, \sigma_{noise}^2\right). \tag{13}$$

As the kernel function that defines the GP prior distribution, the RBF kernel was used. The RBF kernel $k(\theta, \theta')$ is defined as

$$k(\theta, \theta') = \sigma_{signal}^2 \exp\left(-\frac{(\theta - \theta')^2}{2l^2}\right). \tag{14}$$

Here, σ_{signal}^2 denotes the signal variance and l denotes the length scale. The GP hyperparameters,

$$\psi = \left[\sigma_{signal}^2, l, \sigma_{noise}^2\right], \tag{15}$$

were updated by maximizing the log marginal likelihood each time a new data point was added. This procedure enabled the sequential estimation of both the objective-function landscape and the magnitude of the observation noise.

Acquisition function based on EI

The EI is an acquisition function that quantifies the expected amount of improvement over the current best value f_{min} for minimizing the objective function. Using the GP posterior distribution, EI is obtained in closed form as[15,16]

$$EI(\theta) = E\left[\max\left(f_{min} - f, 0\right)\right] = \left(f_{min} - \mu_n(\theta)\right)\Phi(Z) + \sigma_n(\theta)\phi(Z), \tag{16}$$

where

$$f_{min} = \min_{i=1,\ldots,n} f_i, \qquad Z = \frac{f_{min} - \mu_n(\theta)}{\sigma_n(\theta)}. \tag{17}$$

Here, f_i denotes the observed objective-function value at the i-th evaluated gain. $\mu_n(\theta)$ and $\sigma_n(\theta)$ denote the posterior mean and S.D. of the GP at the candidate point θ, respectively. In addition, $\Phi(\cdot)$ and $\phi(\cdot)$ denote the cumulative distribution function and the probability density function of the standard normal distribution, respectively.

Appendix 3

Table 1
Objective-function observations corresponding to the initial best and optimized gains for each participant.

Subject	Selection	K_P [kPa/m]	y
1	Initial best	15436	0.00700
	Optimized	20200	0.00700
2	Initial best	9760	0.00287
	Optimized	9273	0.00236
3	Initial best	19852	0.00569
	Optimized	17229	0.00524
4	Initial best	4583	0.00399
	Optimized	8821	0.00440
5	Initial best	11437	0.00679
	Optimized	20200	0.00571
6	Initial best	6485	0.00749
	Optimized	6965	0.00734
7	Initial best	4733	0.00518
	Optimized	7284	0.00473